UC Merced
UC Merced Previously Published Works

Title

Activation Volume in Shear-Driven Chemical Reactions

Permalink

Journal

ISSN

Authors

Martini, Ashlie
Kim, Seong H

Publication Date

DOI

Activation Volume in Shear-Driven Chemical Reactions

Ashlie Martini[1*] and Seong H. Kim[2*]

1) Department of Mechanical Engineering, University of California Merced, Merced, CA 95343

2) Department of Chemical Engineering and Materials Research Institute, Pennsylvania State University, PA 16802

* Corresponding authors: amartini@ucmerced.edu, shk10@psu.edu

Abstract

Interfacial shear-driven or shear-assisted chemical reactions play an important role in many engineering processes, including reactions between lubricant additives and the surfaces of mechanical components and fabrication of surface topographic features. Mechanistic studies of shear-driven chemical reactions often employ a mechanically assisted thermal-activation model from which a so-called activation volume can be defined. Activation volume is important because it quantifies the efficiency of interfacial shear to drive the reaction. Recent advancements in methods have enabled calculation of activation volume from both nano- and macro-scale experiments as well as simulations. However, the calculated volumes differ by orders of magnitude, even for the same reactant species, and the physical interpretations vary correspondingly. Here, we review how activation volume has been measured and interpreted for shear-driven reactions in the literature with the goal of guiding future efforts to understand and use this important parameter for engineering design through tribochemistry.

1. Introduction

Interfacial shear-driven or shear-assisted chemical reactions, also called tribochemical reactions, are relevant to many manufacturing processes. Such reactions can occur whenever relative motion between surfaces results in shear force on reactant species. Shear force may contribute to vibratory mechanochemical syntheses using ball mills,[1] but the inability to isolate the effects of various mechanical processes occurring at colliding interfaces makes it difficult to estimate how much shear actually contributes. In contrast, the following two types of application-relevant chemical reactions are driven almost entirely by shear: (i) material synthesis leading to growth of deposits or films on surfaces, and (ii) material removal from surfaces resulting in wear or polishing. Although sliding solid surfaces exert both compressive normal stress and tangential shear stress,[2] it is now known that tribochemical reactions do not occur readily without dynamic shear stress.[3] Chemical reactions activated or facilitated by interfacial shear are the subject of this review. Shear force can accelerate reactions directly, as well as indirectly through frictional heating. When the shear rate is high enough that frictional heating is faster than heat dissipation via convection of surrounding fluid or conduction through the contacting solid, thermal reactions may occur. Similarly, if wear is involved, dangling bonds on the worn surfaces might induce chemical reactions. However, this review paper will not cover such indirect processes and the scope is limited to direct mechanical activation.

Shear-driven reactions of lubricant additives at the surfaces of mechanical components are ubiquitous in almost all manufacturing and transportation systems.[4-9] Yet, the chemical additives used in these lubricants have remained essentially the same for decades. For example, the discovery of the most effective antiwear additive, zinc dialkyl dithiophosphate (ZDDP), over 70 years ago was serendipitous.[10, 11] ZDDP was originally developed as an oxidation inhibiting additive, but then was found to form tribo-films with outstanding antiwear properties. It was later shown that the combustion products of ZDDP have negative impacts on catalytic converters used to remove pollutants from exhaust gas.[12] Since then, many studies have tried to replace ZDDP, but the progress has been very slow.[10, 13] This is partially because development of alternatives largely relies on empirical knowledge, rather than *a priori* first principles. Fundamental knowledge of tribochemical mechanisms could significantly accelerate development of lubricant additives.[14]

In semiconductor manufacturing, chemical mechanical polishing (CMP) processes are widely used for planarization of semiconductor device surfaces and smooth finishing of optics

surfaces.[15-17] The tribochemical reactions underlying these processes are facilitated by the mechanical energy of slurry particles sliding on the device surface in solutions containing reactive chemicals.[18] While modern CMP is now a very sophisticated technique, the basic approach is unchanged. Researchers now face new challenges that have arisen due to the fact that many engineering materials are highly sensitive to the chemical environment and mechanical stress associated with CMP itself. Also, pattern dimensions and thicknesses of semiconductor devices are approaching molecular and atomic scales, so CMP will need transformative evolution to planarize surface features of such small scales without leaving surface and sub-surface defects.[19] Thus, there is a fundamental need for scientific advancements to meet current and emerging technological challenges.

Even though these two categories of processes – material growth and material removal – have different physical and chemical mechanisms and their end results are different, they have an important commonality – both types of reactions do not occur in the absence of mechanical stress. Unlike thermal, photochemical, or electrochemical reactions, in which heat, light or electrical bias drives the system toward the transition state of a reaction pathway according to well-developed theories, the mechanisms underlying tribochemical reactions are far less established.[20] This is because tribochemical reactions do not occur under typical thermal reaction conditions; rather, they are driven by sliding solid surfaces, creating transient (dynamic) and non-equilibrium reaction conditions. Conventional chemical reactions are driven by electronic transitions (via vibrational excitations, photon absorption, or electron transfer) at the molecular scale, which are coupled with changes in bond length or angle along a specific reaction coordinate. In tribochemical reactions, bond lengths and/or angles are altered by the mechanical stress exerted by sliding solid surfaces. These alterations are accompanied by or lead to electronic transitions of reactant species. Since tribochemical reactions occur at the interface buried between solid interfaces, it is extremely difficult to use *in-situ* chemical probes to detect and identify intermediate species. Often, these intermediates are released into the bulk phase (surrounding medium) where they are diluted below the detection limit of many characterization methods or undergo secondary reactions forming side products, which limits identification of the fundamental reaction pathways.

A mechanistic understanding of how mechanical shear facilitates interfacial chemical reactions could have a significant impact on both fundamental surface science and engineering

design through tribochemistry. To facilitate the fundamental study of tribochemical mechanisms, this paper provides a critical review of recent findings and interpretations of how shear stress activates chemical reactions at sliding interfaces, with specific emphasis on the parameters that determine by how much or how quickly a reaction can be driven by mechanical stress.

2. Theoretical Framework

Shear-induced tribochemical processes can be understood in the context of transition state theory in which, following the Arrhenius equation, the rate constant of the reaction (k) is exponentially related to the energy barrier that must be overcome for the reaction to proceed. When there is no mechanical force involved, this barrier is the thermal activation energy (E_a). Mechanical force or, more specifically, shear force in a sliding contact, can lower this energy barrier. The potential energy surface (PES) along a hypothetical reaction coordinate is schematically illustrated in Figure 1.[21] This model is often called "mechanically-assisted thermal activation" or "stress-assisted thermal reaction".[22-25] In this model, the effective energy barrier is lowered by the mechanical energy (E_m) provided by the shearing interface (Figure 1). The concept is captured by the following equation that has been widely used in the literature, with some variations:[22-25]

$$k = A \cdot exp\left(-\frac{E_a - E_m}{k_b T}\right) \qquad (1)$$

where k is the rate constant, A is the pre-exponential factor, the unit of which will vary depending on whether the left-hand side of the equation is reaction rate or reaction yield, and k_b and T are the Boltzmann constant (1.38×10^{-23} J/K) and temperature, respectively.
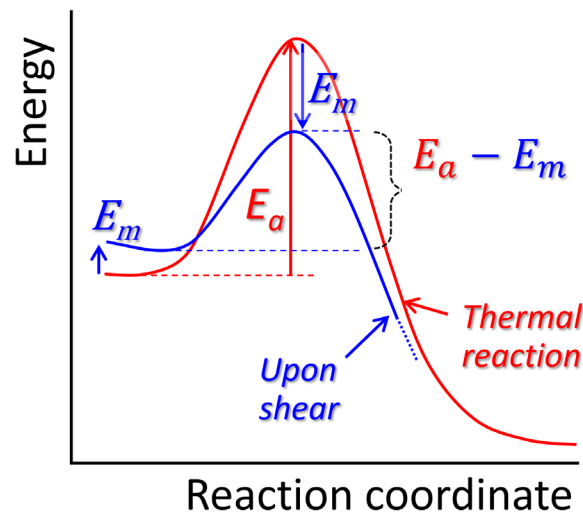
Figure 1: Simplified hypothetical PES for a thermal reaction (red) and a shear-driven reaction (blue). Note that the energy level here is not drawn to scale so the relative magnitudes in this simple schematic diagram should not be interpreted. Also, mechanical activation can occur at either the reactant or transition state, or both. It is not possible to experimentally determine which state is activated; only the net effect can be measured. Further, the tribochemical products may be thermodynamically less stable than the reactants but kinetically stable because the reactants necessary for backward reactions are lost to the surrounding medium and thus not available at the reaction sites. The reaction coordinate is not necessarily the same for the same reaction driven mechanically or thermally.

Many variations of the mechanically assisted thermal activation model have been utilized,[22-25] but all have basically the same form in which the rate of a reaction is an exponential function of the mechanical energy that lowers the thermal activation energy. The E_m term is usually written as shear force, F, multiplied by activation length, Δx^*, or shear stress, τ, multiplied by activation volume, ΔV^*.

$$k = A \cdot exp\left(-\frac{E_a - F \cdot \Delta x^*}{k_b T}\right) = A \cdot exp\left(-\frac{E_a - \tau \cdot \Delta V^*}{k_b T}\right) \tag{2}$$

The terms used to convert force or stress to energy, Δx^* or ΔV^*, are extremely important because they determine the efficiency of the shear action to drive a given reaction, i.e., the amount by which the reaction is accelerated at a given force or stress. In other words, activation length and volume are measures of how applied force distorts the PES, facilitating the transition along the reaction coordinate over an energy barrier that may be too large otherwise. Note that, in the general context of mechanochemistry, force can facilitate or impede a reaction, but cases where force impedes reactions are rare. The form of Eq. (2) assumes that force facilitates the reaction, consistent with the behavior observed for most tribological systems.

Forms of the mechanically-assisted thermal activation model have been proposed that contain a second order term to capture nonlinear effects of force on the PES.[25, 26] Second-order expressions were shown to describe the shear-induced decomposition of adsorbed species on oxidized graphene and formation of tribofilms from ZDDP [25]. Second-order effects can be identified if linear extrapolation of measured rates to the zero-stress limit does not give the activation energy of the reaction. However, since most tribochemical measurements are performed at very high stresses and within relative narrow stress ranges, large extrapolation is required and

there is significant uncertainty associated with calculations of the zero-stress rate. Therefore, it is difficult, in most cases, to determine if second-order effects are present or not.

As such, this review will cover the more commonly used first-order equation. Taking natural logarithm of Eq. (2) gives the following expression:

$$ln(k) = ln(A) - \frac{E_a}{k_bT} + \frac{\Delta x^*}{k_bT}F = ln(A) - \frac{E_a}{k_bT} + \frac{\Delta V^*}{k_bT}\tau \qquad (3)$$

With this formulation, Δx^* or ΔV^* can be quantified from the slope of the semi-log plot of the reaction rate constant versus F or τ, respectively, assuming the rate is measured in conditions where frictional heating is negligible.

3. Magnitude of Activation Volume

3a. Experimental Approaches

In most experimental studies, ΔV^* is determined rather than Δx^*. This is simply because it is not possible to control the force applied along a specific reaction coordinate of a molecule depicted in Figure 1. In most tribo-tests, a pre-set force (F_N) is applied in the direction normal to the sliding interface. If the contacting bodies can be approximated as a sphere in contact with a flat surface, the effective contact area (A_{eff}) can be calculated using contact mechanics,[27] and the normal stress can be defined as $\sigma = F_N/A_{eff}$. For nanoscale contacts, adhesion force is added to the applied force to obtain the total normal load.[27] For macro-scale contacts, the adhesive contribution is negligible and only the applied load needs to be considered in the calculation.[28] Of course, the contact stress obtained in this way is an average; any topographic roughness can alter the local stress within the contact area.

Reactions in sliding interfaces are driven by shear, so the more relevant stress is shear stress (τ) in the tangential direction. The shear stress cannot be measured; it can only be calculated from the measured friction force (F_f). However, this experimental value (F_f) may not be the same as the shear force F in Eq. (3) (discussed in Section 5). Regardless, in an experiment τ is obtained by dividing F_f by A_{eff}: $\tau = F_f/A_{eff}$. Because obtaining accurate A_{eff} during sliding is even more difficult than estimating it for a stationary contact, some studies have used normal contact stress (σ), instead of shear stress (τ) for calculation of ΔV^* using Eq. 3. Other studies have used

Amontons law to approximate $\tau \approx \mu \times \sigma$, where μ is the coefficient of friction (COF). This relationship has recently been proven to be valid within reasonable experimental error for both macroscopic and microscopic contacts (Figure 2).[29] In this recent study, it was shown that, if the surface roughness is smaller than the Hertzian deformation depth and surface roughening due to wear is negligible, the Hertzian contact area can be used for this calculation; if not, the effective contact area should be calculated from the surface roughness of the sliding track or measured independently during sliding.[29]
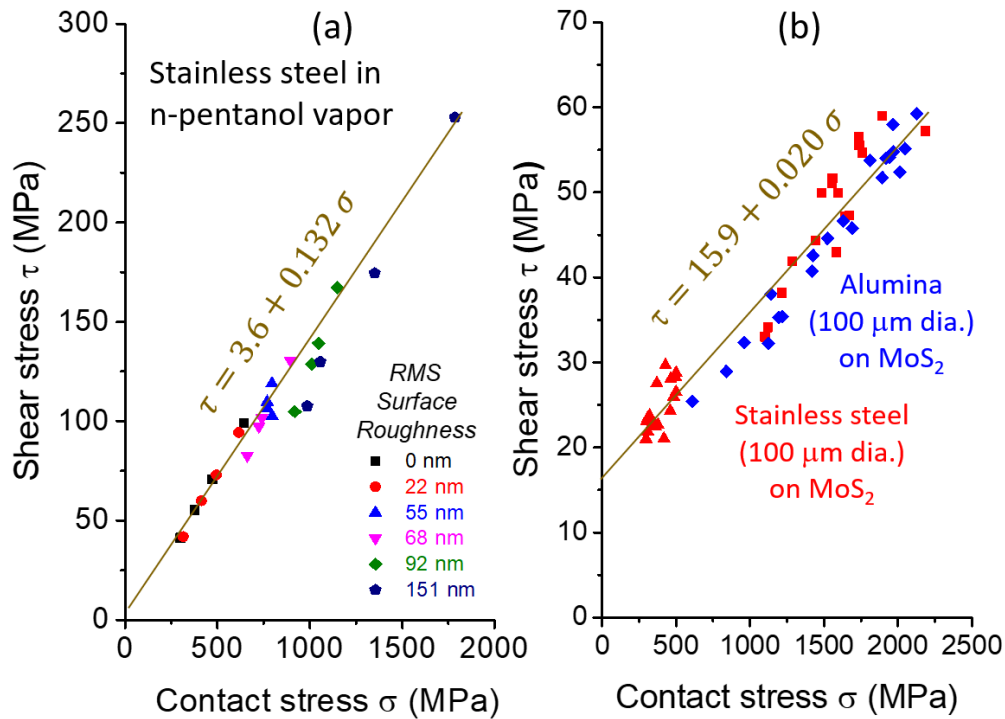

Figure 2. Empirical relationship between the interfacial shear stress (τ) due to kinetic friction and the average normal contact stress (σ) for (a) macroscopic sliding of a 3 mm dia. stainless-steel ball on a stainless-steel surface in n-pentanol vapor phase lubrication condition and (b) microscopic sliding of alumina and stainless-steel spheres (100 μm dia.) on a MoS$_2$ surface. The regression result in (a) confirms that the adhesive contribution (which is the intercept in this plot) is negligible for the macroscale contact, but the data in (b) shows it is significant for the microscale contact. Reproduced with permission from Ref. [29].

Experimental studies have focused on two types of reactions, those that facilitate the removal of material and those that contribute to the growth of a tribo-film. In the material removal case, reaction yield is quantified as the volume of material worn away from the surface being

sheared or rubbed. For the material growth case, yield is measured as the volume or thickness of films as they grow on surfaces. Both removal and growth can be measured using experimental techniques that are readily available within the tribology community, primarily the ball-on-flat apparatus and atomic force microscopy (AFM). Figure 3a shows an example where tribopolymers generated along the sliding track from a ball-on-flat experiment in a vapor phase lubrication condition were imaged with AFM and the total product yield (volume) was calculated from the images. The AFM can also be used as an *in situ* measurement tool for film growth or surface wear by sliding the AFM tip over the surface in contact mode at a high load to drive the reaction and then obtaining a topographic image of the contact-scanned area with tapping mode or contact mode at a light load. This approach enables measurement the yield of the film growth or surface wear reactions as a function of time.
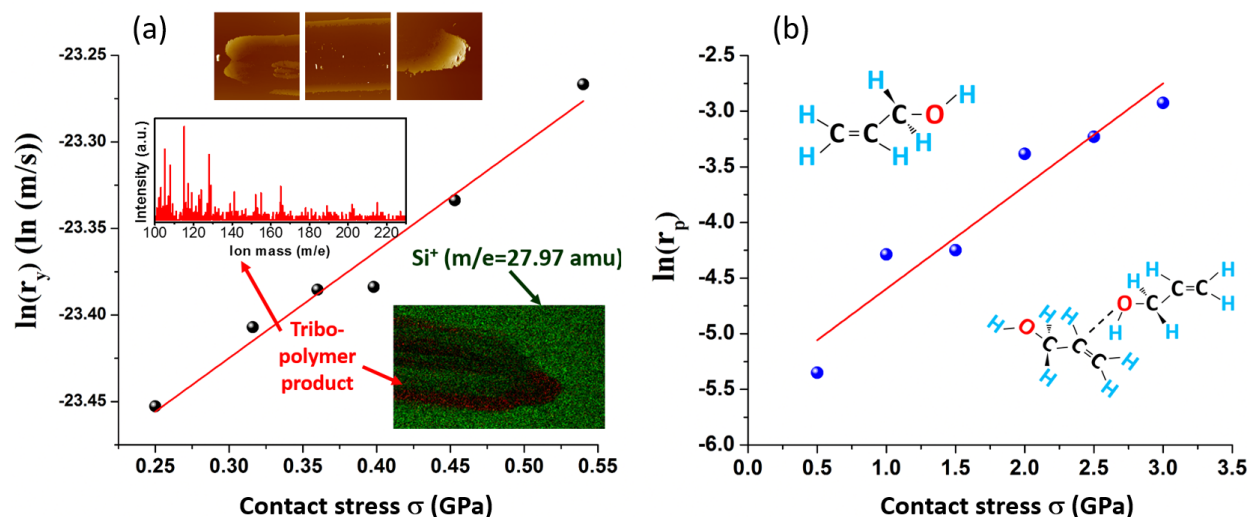

Figure 3: Semi-log plots of tribo-polymerization yield (r_y or r_p) of allyl alcohol on silica as a function of contact stress (σ) obtained from (a) ball-on-flat experiments and (b) reactive molecular dynamics simulations. The activation volume obtained in this work was calculated from the slope assuming $\tau \approx \mu \times \sigma$. Insets in (a) are AFM images and time-of-flight secondary ion mass spectrometry (ToF-SIMS) analysis data of tribo-polymers. Reproduced with Permission from Ref. [30]

In some studies, reaction yield was converted to reaction rate and further to rate constant. This conversion involves dividing the total reaction yield (wear volume or product amount) by the total sliding time. But, it should be noted that, in most experimental conditions, the substrate makes

sliding contact periodically with the counter-surface during the tribo-test because the contact diameter is much smaller (only on order of 10's nm in AFM and 10's-100's μm in ball-on-flat experiments) than the sliding distance of each cycle (typically 100's nm in AFM and in the mm to cm range in ball-on-flat tests). Thus, conversion of measured reaction yield to a reaction rate constant is not as straightforward as in typical reaction kinetics. For that reason, some studies directly used reaction yield in analyses, instead of converting it to a rate constant. However, this does not affect the calculation of ΔV^* from data collected at different applied loads, as long as all other experimental conditions kept constant, because the conversion of reaction yield to rate constant only affects the intercept (pre-exponential factor), not the slope, of the semi-log relationship in Eq. (3).

3b. Simulation-Based Approaches

Theoretical studies using atomistic methods, either density functional theory (DFT) or reactive molecular dynamics (MD) simulations, can be used to complement experiments and explore the atomic- and molecular-scale mechanisms underlying tribochemical reactions. These approaches reveal the fundamental pathways of shear-driven reactions as well as provide alternative ways to investigate the meaning of activation length or volume.

DFT calculations of tribochemistry typically involve a model molecule interacting with an ideal crystalline surface. Energy optimization is performed at each step in a reaction to identify pathways and calculate the associated energies. DFT is often used in conjunction with nudged elastic band (NEB); in this case, the initial and final states are identified using DFT and then NEB is used to identify the intermediate states.[31-33] The result is energy as a function of reaction coordinate, such as that shown in Figure 4, from which the activation energy (the energy difference between the transition state and the initial state) can be obtained. This approach can be used to calculate activation length or volume using models of reactant species of interest on surfaces or confined between two solid slabs. In the latter case, the distance between the slabs is incrementally decreased to apply normal load,[34, 35] as shown in the example in Figure 5. A similar process can be carried out to model shear stress by incrementally moving one of the slabs laterally.[36] At each slab-slab distance, the reaction energy is calculated. Then, activation length can be obtained from a linear fit of reaction energy as a function of force,[31, 35] or, similarly, the activation volume can be obtained from a linear fit of energy as a function of pressure.[37]
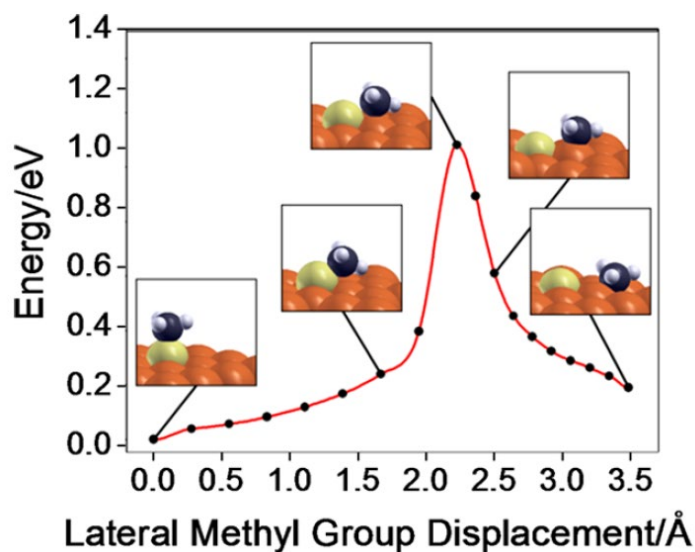
Figure 4: Potential energy profile for the lateral displacement of the methyl group in methyl thiolate, for the decomposition of methyl thiolate species on a Cu(100) surface obtained using DFT calculations. Reprinted with permission from Ref. [31]
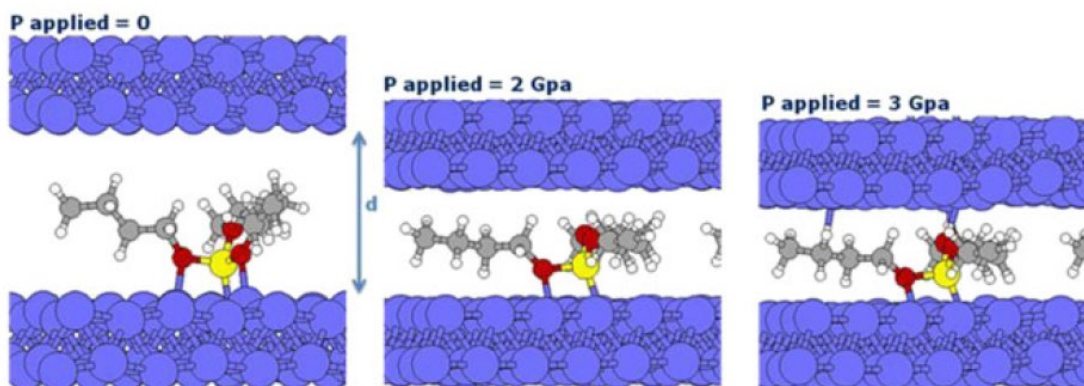

Figure 5: DFT-based calculation of tributylphosphite molecules between Fe(110) surfaces at different normal stresses ("P applied" in this figure). Reprinted with permission from Ref. [34]

DFT calculations provide detailed information about the reaction pathway and energetics. However, they are limited in the size scale, i.e., number of atoms, that can be modeled, and they do not capture dynamic effects, such as transient impact forces between asperities, that may play an important role in tribochemical reactions. The computational expense of DFT also precludes its use to study reactions with many different potential pathways. Finally, amorphous surfaces that might be the initial state of a solid substrate or evolve during the reaction due to subsurface

deformation induced by friction are not easily modeled using DFT. An alternative is reactive MD simulations. The term reactive here refers to the functional form of the empirical potential, or force field, that can capture the formation and breaking of chemical bonds. MD simulations with reactive potentials are used to study tribochemical reactions by modeling the molecules of interest confined between two walls of material and then imposing normal force and/or sliding of one of the walls. MD can model much larger systems than DFT and can readily be used to track and differentiate multiple possible reaction pathways for materials from crystalline to amorphous. Such simulations can also be performed at various temperatures to differentiate thermally and mechanically driven reactions. Reaction yield is typically quantified in terms of number of bonds broken or formed, or the number of reactants consumed and/or products formed in the system.

Activation length or volume can be calculated in various ways from reactive MD simulations. First, reaction yield can be fit to Eq. (3), following the same procedure as used in experimental studies. This approach is advantageous because it enables direct comparison between simulations and experiments, as shown in Figure 3, despite the large difference in size- and time-scale between them.[30] Second, for a given reaction pathway, the change in molecular volume accompanying key steps in the reaction can be directly calculated from changes in atom positions.[38] This approach is useful because it can potentially provide insight into the physical meaning of the activation volume term. However, there is uncertainty in results obtained using this approach because they are highly sensitive to which atoms are used in the calculation and a large variance is possible from molecule to molecule due to the stochastic nature of the simulation. Lastly, representative molecules can be extracted from the dynamic simulations before and after a given reaction. These "snapshots" can then be used as the initial and final states for NEB calculations.[39] NEB calculations generate potential energy profiles, such as those shown in Figure 6, and identify energy barriers and the transition state of the reaction which, as mentioned above, is important for understanding ΔV^*.
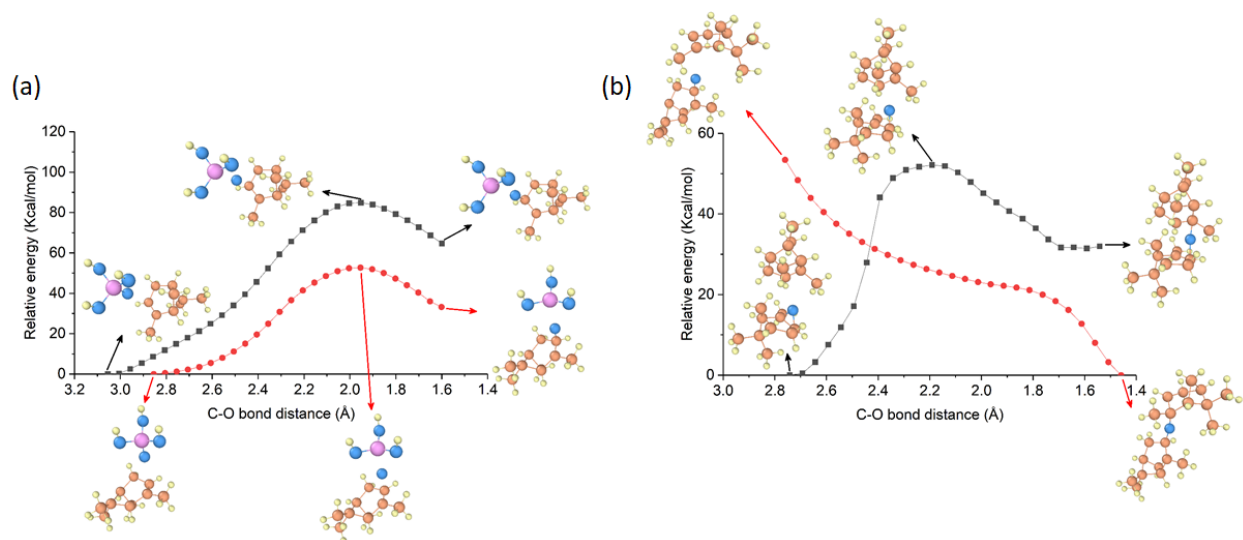
Figure 6: NEB calculations based on a reactive empirical force field provide the relative potential energy for (a) oxidative chemisorption of α-pinene on an SiO₂ surface and (b) association of intermediate species with α-pinene, in the relaxed state (black) and deformed by shear (red). Adapted with permission from Ref. [39].

4. The magnitude of activation volume

4a. Magnitudes of Reported Activation Volumes

Tables 1 and 2 summarize over 40 references that reported the magnitude of activation volume ΔV^* or, in some cases, activation length Δx^*. Table 1 lists studies of shear-driven material removal, i.e., wear, and Table 2 lists studies of shear-driven synthesis, i.e., tribofilm growth. The activation volumes or lengths were calculated from experiments, typically either ball-on-flat or AFM, or atomistic simulations, either DFT or reactive MD, using the methods described in Section 3. Note that some studies used shear stress (τ), while others considered normal stress (σ) to calculate the activation volume. Thus, when these two values are to be compared, the magnitude of COF should be considered as a correction factor.[29] To be dimensionally correct, ΔV^* or Δx^* in Eq. (3) should be reported in units of volume or length per molecule; if the gas constant (R = 8.314 J/mol·K) is used instead of the Boltzmann constant (k_b) in Eq. (3), then ΔV^* or Δx^* should be volume or length per mole. While this gives a physical dimension per molecule or mole of reactants for tribofilm formation (Table 2), it is difficult to define the reacting unit in the case of material removal (Table 1). Therefore, here we report ΔV^* or Δx^* simply as volume or length, as reported in the original papers.

12

Table 1. Activation volume ΔV^* (Å^3) or length Δx^* (Å) reported for *material removal* processes in the literature. The last column shows the interpretation of the physical meaning of the physical meaning of ΔV^* or Δx^* proposed in each paper as discussed in Section 4; here, "-" indicates that no physical meaning was suggested.

System Studied		ΔV^* or Δx^*	Method	τ/σ	Meaning
Dissociation of OH and C-O-C on graphene[40]	Original	11±2	AFM	σ	Atomic Size
	Re-analysis[25]	50±20			
Wear of calcite by Si$_3$N$_4$ in CaCO$_3$ solution[41, 42]		37±3 44±4	AFM	σ	Atomic Size
Wear of Si tip sliding on polymer[43]		55±35	AFM	σ	Atomic Size
Wear of Si-DLC by SiO$_2$ tip[44]		340±200	AFM	σ	Atomic Size
Wear of a-C:H DLC tip sliding on UNCD[45]		5.5±0.8	AFM & MD	σ	Atomic Size
Wear of Si tip on diamond[46]	Original	6.7±0.3	AFM	σ	Atomic Size
	Re-analysis[47]	6.7 to 120			
Wear of NaCl step edge by Si$_3$N$_4$[48]		86±6	AFM	σ	Atomic Size
Wear of a-C by Al$_2$O$_3$ ball[49]		5.6±0.7	Ball-on-Flat	σ	Atomic Size
Wear of Si wafer by SiO$_2$ sphere[50]	SiO$_x$	45±5	Microsphere	σ	-
	Si/H	28±3			
H-terminated Si(100) by silica sphere in air[51]		33	Microsphere	σ	-
Si wafer by silica in water[52, 53]	Si(100)	115±10	Microsphere	τ	-
	Si(110)	72±2			
	Si(111)	87±6			
AFM wear of Si wafer[54]	Al$_2$O$_3$ tip	58±3	Microsphere	τ	Deformation
	SiO$_2$ tip	60±4			
Si wafer by silica in humid air[55]		38±3	Microsphere	τ	
Slab-on-slab contact of silica polymorphs (β-cristobalite or α-quartz)[56]	β-c (001)	84±3.3	DFT	σ	Deformation
	β-c (111)	30±3.3			
	β-c (111)	-5±3.3			
	α-q (0001)	18±3.3			
Wear of GaAs by SiO$_2$ in 40% RH[57]		72±10	Microsphere	τ	Deformation
Wear of oxidized graphene by Si tip[58]		30±15	AFM	σ	-
Wear of oxidized DLC surface by Si tip[59]		10.8±0.2	AFM	σ	-
Decomposition of CH$_3$S from Cu(100)[31]		2.2 (Δx^*)	DFT	τ	-

Methyl thiolate species adsorbed on Cu (100)[60]	46±1	AFM	σ	-
	0.31±0.03 (Δx^*)	DFT	σ	-
Dissociation of TMPi and TBPi on iron[34]	3.0 (Δx^*)	DFT	σ	Deformation
Perfluoropolyether in diamond interface[61]	25	MD	τ	

Table 2. Activation volume ΔV^* (Å^3) or length Δx^* (Å) reported for *tribofilm growth* processes in the literature. The last column shows the interpretation of the physical meaning of the physical meaning of ΔV^* or Δx^* proposed in each paper as discussed in Section 4; here, "-" indicates that no physical meaning was suggested.

System Studied		ΔV^* or Δx^*	Method	τ/σ	Meaning
ZDDP tribo-film in boundary regime[62]	Original	3.8±1.2	AFM	σ	Atomic Size
	Re-analysis[25]	80±20			
ZDDP tribo-film in full film regime[63]	Original	180	Ball-on-Flat	τ	Atomic Size
	Re-analysis[25]	200±30			
ZDDP tribo-film in full film regime[3]	Primary	125	Ball-on-Flat	τ	-
	Secondary	150			
Manganese phosphate[64]		52	Ball-on-Flat	τ	-
Allyl alcohol on hydroxylated SiO$_2$[30]		7.8±0.6	Ball-on-Flat	τ	Deformation
		11	MD		
Allyl alcohol and H$_2$O on SiO$_2$[65]		5.8±1.1	Ball-on-Flat	τ	-
α-pinene on dehydroxylated SiO$_2$[38]		8.3±0.7	Ball-on-Flat	τ	Deformation
		6	MD		
Polymerization on stainless steel[66]	α-pinene	8.2±0.6	Ball-on-Flat	τ	Deformation
	pinane	21.9±0.7			
	n-decane	33±3			
α-pinene on different surfaces[67]	Copper oxide	5.8±1.0	Ball-on-Flat	τ	Deformation
	Stainless steel	8.7±0.9			
	Nickel oxide	9.3±1.7			
	Silicon oxide	12.4±2.1			
Cyclopropane carboxylic acid in PAO4 [68]		3300	Ball-on-flat	τ	Deformation
ZDDP film growth[69, 70]		53	Ball-on-Flat	τ	-
Additives in PAO on AISI 52100[71]	ZDDP	0.2 (Δx^*)	AFM	σ	-
	DDP	0.8 (Δx^*)			

4b. Interpretations of the Magnitude of Activation Volume

The first key observation from this summary of previous studies (Tables 1 and 2) is that the *magnitude of ΔV^* varies by orders of magnitude* from study to study, from about 3 $Å^3$ to 300 $Å^3$, for both material removal and growth cases. This range does not appear to be attributable to different size-scales of the measurements nor to differences in molecular species. For example, ΔV^* for growth of ZDDP films ranges from 0.2 $Å^3$ to 180 $Å^3$ (Figure 7).[62, 63] Likewise, ΔV^* for wear of a silicon AFM tip ranges from 6.7 $Å^3$ to 55 $Å^3$.[43, 46] It has also been shown that ΔV^* depends on the direction of sliding relative to the crystallographic orientation of the surface being worn,[52, 53] and on the molecular structure of the reactant species from which films are grown.[66] For the same molecule, the ΔV^* also varies depending on the reactivity of the substrate on which the molecule is being sheared.[67] The reason for the differences or similarities between activation volumes may vary depending on the physical meaning of ΔV^* itself.
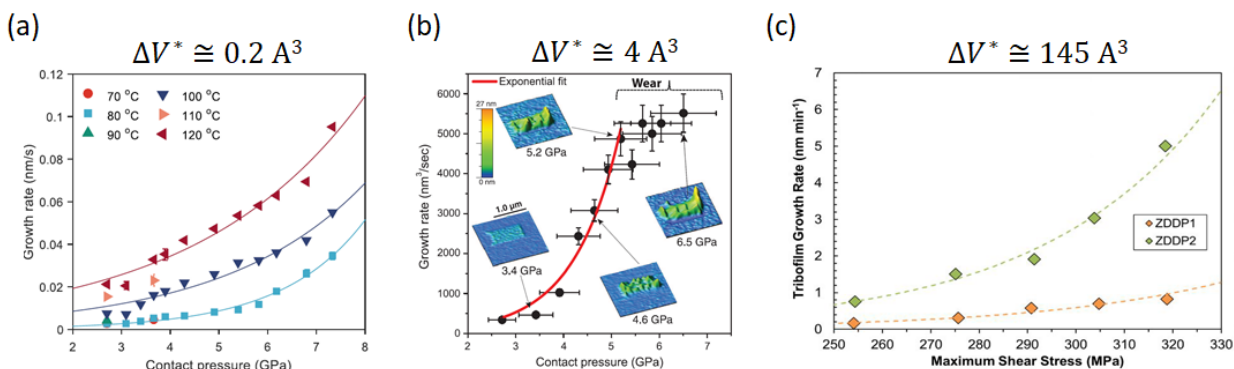

Figure 7: Activation volume (given above each figure) calculated by fitting experimental ZDDP film growth rate data to Eq. (3) (or similar) from three different recent studies. (a) Rate of ZDDP film growth measured using AFM as a function of contact pressure (normal stress) at different temperatures. Reprinted with permission from Ref. [71]. (b) ZDDP film growth rate measured using AFM with insets showing AFM images of the film at different contact pressures. Reprinted with permission from Ref. [62] (c) Rate of film growth for a C_8 primary branched alkyl (ZDDP1) and a C_6 secondary alkyl (ZDDP2) measured using a ball-on-flat experiment in the elastohydrodynamic lubrication regime. Reprinted with permission from Ref. [3].

Another important observation is that ΔV^* has been calculated from either normal or shear stress. A recent experimental study of ZDDP film formation showed definitively that shear stress

(τ) is the key factor in driving tribo-film growth reactions.[3] However, the controllable parameter in most experiments is normal stress (σ), which can be calculated by dividing the applied load by the contact area. In some studies, shear and normal stresses were assumed to be linearly related via COF as $\tau = \tau_0 + \mu\sigma$, where τ_0 is the shear stress at zero load that is particularly relevant for nanoscale contacts where adhesion plays a significant role.[72, 73] If μ is constant, this relationship can be used to calculate ΔV^* from Eq. (3) using σ. However, the magnitude of μ may change during a test, especially at the beginning, due to wear or film growth that change the frictional characteristics of the sliding interface [38, 65, 67]. Therefore, ΔV^* calculated using σ, even if it is converted to τ using μ as a proportionality constant, may or may not be accurate, depending on the material system and operating conditions.[65, 74]

Lastly, careful analysis of the literature reveals discrepancies in the proposed physical meaning of the ΔV^* term. The most frequently suggested interpretations are based on comparisons between the magnitude of the fit value and some length scale that is characteristic of the system being studied. Particularly, the physical meaning of ΔV^* is most often interpreted as the size of individual atoms, ions or bonds.[40-46, 48, 49, 62] Similarly, studies that extract larger magnitudes of ΔV^* sometimes correlate their values with molecular size scales, i.e., the area of a molecule onto which frictional force is imparted times the distance through which such a force acts.[63] An alternative interpretation of activation volume is related the degree of physical deformation of reactant species from their thermal equilibrium geometry. In this case, ΔV^* could be correlated to changes in volume or bond length due to deformation of molecular species.[30, 34, 38] Such deformation would play critical roles in activating reaction pathways that are not accessible thermally.

5. Perspectives

Based on the conceptual energy diagram described in Figure 1, $\Delta V^* \cdot \tau$ or $\Delta x^* \cdot F$ could be interpreted as the amount of mechanical energy that effectively lowers the thermal activation energy barrier at the transition state along the reaction coordinate (for example, Figure 6a). Or it could be effectively increasing the reactant energy state (for example, Figure 6b). The product state may be less stable than the reactant state (for example, Figure 4), but it can still be kinetically stable since chemical species needed for the reverse reaction to occur are lost into the surrounding

medium. Regardless, most studies reviewed in this article have reported an exponential dependence of tribochemical reaction yield or rate on applied stress or force. Thus, the mechanical activation contribution appears in the exponent term of Eq. (1), where it effectively reduces the activation energy barrier for the reaction. To be dimensionally consistent in Eq. (2), the proportionality constant describing the linear relationship between the logarithmic reaction yield or rate and the applied stress (τ) or force (F) should have the dimension of volume (ΔV^*) or length (Δx^*), respectively. This kinetics argument is mathematically solid, but it does not provide any atomistic or molecular meaning for the proportionality constant. Unfortunately, at this point, there is no consensus in the published literature about either the magnitude or the physical/mechanistic meaning of ΔV^* (or Δx^*). The following are some thoughts on this topic which might explain the discrepancies and potentially lead to their resolution going forward.

Let's consider a simple one-dimensional reaction coordinate along a specific bond axis (x) and assume that the applied shear force (F) lowers the energy state along this coordinate in proportion to the deviation from the equilibrium bond length.[21] In this picture, it is conceptually easy to visualize that the activation length would be the difference between the bond length at the transition state (x_{tr}) and the equilibrium distance (x_{eq}), i.e., $\Delta x^* = x_{tr} - x_{eq}$, and the activation barrier is lowered by $\Delta x^* \cdot F$ at the transition state. However, this picture does not describe how shear force is transferred to the specific reaction path of a reactant molecule. The simple 1D model cannot capture the full dynamics of a reaction involving multiple variables, i.e., more than just a bond length or angle as a single descriptor. It also does not resolve key questions about the process. For example, how much of the applied force is dissipated via elastic deformation of the substrate or consumed for lateral shear of the interface? And, importantly, what portion of the interfacial force is effectively channeled into the reaction coordinate?

The experimentally measured friction force (F_f) will be the sum of all possible physical and chemical contributions.[75-77] Chemical contributions to friction might include hydrogen bonding interactions or transient chemical bond formation / dissociation,[75-77] while examples of physical contributions are stick-slip type processes,[78] plastic deformation,[79] or fluid shear.[80, 81] When the experimentally measured friction is used in Eq. (3), the implicit assumption is $F=F_f$, i.e., friction is mainly due to chemical reactions occurring in the sliding interface. However, this can result in an over- or under-estimate of ΔV^* obtained by fitting to Eq.

(3). For example, if the physical contribution to the measured friction force is more significant than the chemical contribution, using the experimental value F_f as F in Eq. (3) may result in an under-estimation of the magnitude of ΔV^*.

Another factor that could affect activation volume obtained from experimental fitting is the efficiency of transferring or channeling shear stress along the reaction coordinate. This efficiency could be very different from one experiment from another, leading to a large discrepancy in activation volumes for the same or similar tribochemical reaction. This might explain why the activation volumes for ZDDP film formation in boundary versus hydrodynamic lubrication conditions were so different (Figure 7). In a study of cyclopropane carboxylic acid in PAO4,[68] it was speculated that tribochemical reactions took place mostly at asperity contacts where flash temperature and pressure were significantly higher than in the hydrodynamic (liquid film) lubrication region. The shear stress at the asperity contacts is likely to be much larger than the average shear stress across the sliding contact area, which might explain the very large activation volume estimated from the average shear stress in Ref. [68] (Table 2).

In this context, one may not be able to directly compare the absolute magnitudes of ΔV^* obtained using different instruments or under different conditions – such as nano-scale vs. macro-scale measurements or boundary lubrication vs. hydrodynamic lubrication experiments. Nonetheless, it would be still meaningful to compare relative magnitudes of ΔV^* calculated for a series of analogous systems – such as reactivities of similar precursor molecules on a given surface [66] or reactivities of certain surfaces for a certain reaction of the same precursor molecule [67, 74] – determined under constant or reasonably similar frictional conditions.

Although activation volume or length is calculated from the slope of $ln(k)$ vs. τ relationship in Eq. (3), the intercept of this equation is also relevant. In Eq. (3), one can also see that the intercept is a function of the thermal activation energy (E_a). Therefore, if the tribochemical rate constant with the correct unit is used on the left-hand side of Eq. (3), the thermal activation energy in the absence of shear can be estimated from the intercept. In the previously mentioned study of carbon tribofilm formation from cyclopropane carboxylic acid in PAO4 [68], it was shown that the activation energy estimated by extrapolation to zero-shear stress was very close to the thermal activation energy of C-C dissociation in cyclopropane (Figure 8a).
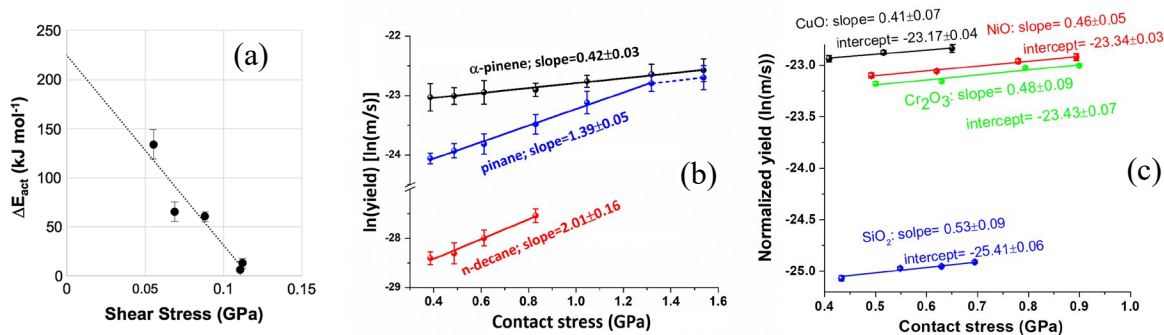
Figure 8: (a) Relationship between activation energy for tribofilm formation from cyclopropane carboxylic acid in PAO4 and the shear stress approximated by multiplying the normal contact stress by the steady-state coefficient of friction [68]. (b) Normal contact stress dependence of tribo-polymer yield for α-pinene (black), pinane (blue), and n-decane (red) on stainless steel [66]. (c) Normal contact stress dependence of the tribo-polymerization yield for α-pinene on copper (black), nickel (red), stainless steel (green), and silicon oxide (blue) substrates [67]. Reprinted with permission from Ref. [68] and redrawn from Refs. [66] and [67].

If the reaction rate or yield, instead of rate constant, is used on the left-hand side of Eq. (3), only the relative magnitude of the intercept can be compared for a series of homologous systems. For example, in a study comparing the molecular structure dependence of tribopolymerization of C10 hydrocarbons on a stainless-steel surface [67], thermodynamically more stable molecules exhibited smaller intercept values (which means larger E_a in Eq. (3)), as shown in Figure 8b, while the COFs of the tested molecules were comparable. Similarly, a surface chemistry dependence study of α-pinene tribopolymerization (Figure 8c) showed that the intercept of the $ln(k)$ vs. τ plot was smaller for surfaces with lower catalytic activities (thus larger E_a) [68]. These results confirm that the intercept of the $ln(k)$ vs. τ plot is closely related to the thermal activation energy, i.e., how easily the reaction can occur at zero stress. Figures 8b and 8c also show that, within homologous series, the slope is larger (i.e., larger ΔV^*) for systems with smaller intercept (i.e., larger E_a and lower intrinsic reactivity). This phenomenon is called kinetic compensation and is often observed in surface reactions relevant to heterogeneous catalysis [82]. Then, a larger ΔV^* could mean that the reaction needs more mechanical assistance ($-E_m$) to occur because the E_a under stress-free conditions is larger.

If reaction yield is obtained from an experiment, mathematically, one can simply divide the total yield by sliding time and reactant concentration to get a rate constant. Although this approach is dimensionally correct, it does not necessarily give a physically meaningful and accurate rate

constant. The first issue is determining the concentration. One possible approach is to simply use the concentration in the bulk phase (for example, ZPPD concentration in the lubricant oil or vapor pressure in the environment gas). However, a key difference between tribochemical reactions and thermal reactions is that, in tribochemical reactions, the volume concentration of reactants in the surrounding medium (either liquid or gas phase) is not the concentration of reactants sheared in the sliding contact. The actual concentration will vary depending on the adsorption isotherm of reactive species to the substrate or counter-surface (or both), and the availability of adsorption sites may change as the reaction progresses. The second issue is determining sliding time. The reactants or intermediate species adhered to the substrate are subject to shear intermittently because the contact diameter is smaller than the sliding distance. In such cases, would the total sliding time be appropriate for calculating reaction rate? Or should it be the net time during which the surface species at a given site on the surface are in contact with the counter-surface? This choice is further complicated by the fact that reactive species may desorb from the surface when they are not in contact with the counter-surface between sliding passes? These uncertainties make it difficult to accurately convert reaction yield to a rate constant.

All the calculations of activation volume or length from fitting discussed so far assume that mechanochemical reactions depend exponentially on stress. However, several studies have reported a linear dependence of mechanochemical reactions on applied stress [83-85], which cannot be explained with the Arrhenius-type kinetics discussed in Section 2. This trend cannot be fully explained with the mechanically assisted thermal activation model (Figure 1), suggesting that more complicated mechanisms may play dominant roles for some reaction systems or conditions. In such cases, activation volumes obtained by fitting to the exponential functions would not be physically meaningful.

Finally, empirical data alone cannot determine what specific reaction pathway is activated by the mechanical shear and how it happens; thus, it is difficult to correlate a calculated ΔV^* to a specific physical parameter involved in the shear-induced mechanical activation process. In contrast, computational approaches can calculate the energy levels of specific reactant and transition states with and without a mechanical force applied along a specific reaction coordinate; thus, they can calculate $E_a - E_m$ for a specific reaction. But, without experimental verification of the computational result, it is difficult to judge if the reaction path considered in computations is the dominant mechanism observed in experimental conditions. This limitation can be overcome if

the experimental and computational results are cross validated. Since computational approaches are necessarily molecular scale, it is difficult to make direct, quantitative comparison between experiments and simulations. However, comparisons can still be made for the stress-dependence of reaction yield (for example, Figure 3).[30, 38] To enable experiments and simulations to be used together to understand activation volume, the chemical species and shear conditions must be designed collaboratively such that both experiments and simulations are measuring a quantity that can be compared accurately and meaningfully.

At the start of this review, we described activation volume (ΔV^*) or activation length (Δx^*) as measures of the efficiency of shear stress or force to drive a reaction. This is an important concept because it implies a way to tune tribochemical reactions. A shear-driven reaction system includes the reactant species, the applied force, and the surfaces and/or fluid that transmits the applied force to the reactants. This suggests that, for a given applied force, the reactant/surface system, which determines activation volume or length, could be controlled to manipulate reactivity. However, realizing this possibility requires understanding how shear drives a given reaction, e.g., how shear accelerates a reaction along the thermal pathway or opens new reaction pathways. Similarly, defining the reaction coordinate for shear-driving reactions is critical. Recent advancements in experimental and computational research dedicated to this topic, as summarized in this review, are bringing researchers closer to understanding the fundamental mechanisms of shear-driven reactions and, ultimately, using that information to guide engineering design through tribochemistry.

References

[1] Do, J., Friscic, T. Mechanochemistry: A Force of Synthesis. Acs Central Science 3:13-19 (2017).
[2] Gates, R.S., Hsu, M., Klaus, E.E. Tribochemical Mechanism of Alumina With Water. Tribology Transactions 32:357-363 (1989).

[3] Zhang, J., Ewen, J.P., Ueda, M., Wong, J.S.S., Spikes, H.A. Mechanochemistry of Zinc Dialkyldithiophosphate on Steel Surfaces under Elastohydrodynamic Lubrication Conditions. ACS Applied Materials & Interfaces 12:6662-6676 (2020).

[4] Zhou, Y., Leonard, D.N., Guo, W., Qu, J. Understanding Tribofilm Formation Mechanisms in Ionic Liquid Lubrication. Scientific Reports 7:8426 (2017).

[5] Shimizu, Y., Spikes, H.A. The Tribofilm Formation of ZDDP Under Reciprocating Pure Sliding Conditions. Tribology Letters 64:46 (2016).

[6] Morina, A., Neville, A. Understanding the composition and low friction tribofilm formation/removal in boundary lubrication. Tribology International 40:1696-1704 (2007).

[7] Komvopoulos, K., Li, H. The Effect of Tribofilm Formation and Humidity on the Friction and Wear Properties of Ceramic Materials. Journal of Tribology 114:131-140 (1992).

[8] Equey, S., Roos, S., Mueller, U., Hauert, R., Spencer, N.D., Crockett, R. Tribofilm formation from ZnDTP on diamond-like carbon. Wear 264:316-321 (2008).

[9] Fujita, H., Spikes, H.A. The formation of zinc dithiophosphate antiwear films. Proceedings of the Institution of Mechanical Engineers, Part J: Journal of Engineering Tribology 218:265-278 (2004).

[10] Spikes, H. The History and Mechanisms of ZDDP. Tribology Letters 17:469-489 (2004).

[11] Fields, S. ZDDP: Going, going...or not? Tribology & Lubrication Technology 61:24-30 (2005).

[12] Guinther, G.H., Danner, M.M. Development of an Engine-Based Catalytic Converter Poisoning Test to Assess the Impact of Volatile ZDDP Decomposition Products from Passenger Car Engine Oils. SAE Transactions 116:1003-1012 (2007).

[13] Spikes, H.A. Beyond ZDDP. Lubrication Science 20:77-78 (2008).

[14] de Barros'Bouchet, M.I., Martin, J.M., Le-Mogne, T., Vacher, B. Boundary lubrication mechanisms of carbon coatings by MoDTC and ZDDP additives. Tribology International 38:257-264 (2005).

[15] Wang, Y.G., Zhang, L.C., Biddut, A. Chemical effect on the material removal rate in the CMP of silicon wafers. Wear 270:312-316 (2011).

[16] and, J.J.S., Boer, M.P.d. IC-Compatible Polysilicon Surface Micromachining. Annual Review of Materials Science 30:299-333 (2000).

[17] Hetherington, D., Sniegowski, J.: Improved polysilicon surface-micromachined micromirror devices using chemical-mechanical polishing. SPIE, (1998)

[18] Fischer, T.E. Tribochemistry. Annual Review of Materials Science 18:303-323 (1988).

[19] Krishnan, M., Nalaskowski, J., Cook, L. Chemical Mechanical Planarization: Slurry Chemistry, Materials, and Mechanisms. Chemical Reviews 110:178-204 (2010).

[20] Martini, A., Eder, S.J., Dörr, N. Tribochemistry: A Review of Reactive Molecular Dynamics Simulations. Lubricants 8:44 (2020).

[21] Beyer, M.K. The mechanical strength of a covalent bond calculated by density functional theory. The Journal of Chemical Physics 112:7307-7312 (2000).

[22] Jacobs, T.D.B., Gotsmann, B., Lantz, M.A., Carpick, R.W. On the Application of Transition State Theory to Atomic-Scale Wear. Tribology Letters 39:257-271 (2010).

[23] Spikes, H., Tysoe, W. On the Commonality Between Theoretical Models for Fluid and Solid Friction, Wear and Tribochemistry. Tribology Letters 59:21 (2015).

[24] Spikes, H. Stress-augmented thermal activation: Tribology feels the force. Friction 6:1-31 (2018).

[25] Tysoe, W. On Stress-Induced Tribochemical Reaction Rates. Tribology Letters 65:48 (2017).

[26] Konda, S., Brantley, J., Bielawski, C., Makarov, D. Chemical reactions modulated by mechanical stress: Extended Bell theory. Journal of Chemical Physics 135 (2011).

[27] Jacobs, T., Martini, A. Measuring and Understanding Contact Area at the Nanoscale: A Review. Applied Mechanics Reviews 69 (2017).

[28] Ciavarella, M., Joe, J., Papangelo, A., Barber, J.R. The role of adhesion in contact mechanics. Journal of The Royal Society Interface 16:20180738 (2019).

[29] He, X., Liu, Z., Ripley, L.B., Swensen, V.L., Griffin-Wiesner, I.J., Gulner, B.R., et al. Empirical relationship between interfacial shear stress and contact pressure in micro- and macro-scale friction. Tribology International 155:106780 (2021).

[30] Yeon, J., He, X., Martini, A., Kim, S.H. Mechanochemistry at Solid Surfaces: Polymerization of Adsorbed Molecules by Mechanical Shear at Tribological Interfaces. ACS Applied Materials & Interfaces 9:3142-3148 (2017).

[31] Adams, H., Miller, B.P., Kotvis, P.V., Furlong, O.J., Martini, A., Tysoe, W.T. In Situ Measurements of Boundary Film Formation Pathways and Kinetics: Dimethyl and Diethyl Disulfide on Copper. Tribology Letters 62:12 (2016).

[32] Righi, M., Loehle, S., Bouchet, M., Philippon, D., Martin, J. Trimethyl-phosphite dissociative adsorption on iron by combined first-principle calculations and XPS experiments. RCS Advances 5:101162-101168 (2015).

[33] Righi, M., Loehle, S., Bouchet, M., Mambingo-Doumbe, S., Martin, J. A comparative study on the functionality of S- and P-based lubricant additives by combined first principles and experimental analysis. RCS Advances 6:47753-47760 (2016).

[34] Loehlé, S., Righi, M.C. First principles study of organophosphorus additives in boundary lubrication conditions: Effects of hydrocarbon chain length. Lubrication Science 29:485-491 (2017).

[35] Boscoboinik, A., Olson, D., Adams, H., Hopper, N., Tysoe, W. Measuring and modelling mechanochemical reaction kinetics. Chemical Communications 56:7730-7733 (2020).

[36] Loehle, S., Righi, M. Ab Initio Molecular Dynamics Simulation of Tribochemical Reactions Involving Phosphorus Additives at Sliding Iron Interfaces. Lubricants 6 (2018).

[37] Li, Z., Szlufarska, I. Physical Origin of the Mechanochemical Coupling at Interfaces. Physical Review Letters 126 (2021).

[38] Khajeh, A., He, X., Yeon, J., Kim, S.H., Martini, A. Mechanochemical Association Reaction of Interfacial Molecules Driven by Shear. Langmuir 34:5971-5977 (2018).

[39] Rafatijo, H. Computing activation energies of non-thermal reactions. Molecular Physics (2020).

[40] Felts, J.R., Oyer, A.J., Hernández, S.C., Whitener Jr, K.E., Robinson, J.T., Walton, S.G., et al. Direct mechanochemical cleavage of functional groups from graphene. Nature Communications 6:6467 (2015).

[41] Park, N.S., Kim, M.W., Langford, S.C., Dickinson, J.T. Atomic layer wear of single-crystal calcite in aqueous solution using scanning force microscopy. Journal of Applied Physics 80:2680-2686 (1996).

[42] Dickinson, J.T., Park, N.S., Kim, M.W., Langford, S.C. A scanning force microscope study of a tribochemicalsystem: stress-enhanced dissolution. Tribology Letters 3:69-80 (1997).

[43] Gotsmann, B., Lantz, M.A. Atomistic Wear in a Single Asperity Sliding Contact. Physical Review Letters 101:125501 (2008).

[44] Bhaskaran, H., Gotsmann, B., Sebastian, A., Drechsler, U., Lantz, M.A., Despont, M., et al. Ultralow nanoscale wear through atom-by-atom attrition in silicon-containing diamond-like carbon. Nature Nanotechnology 5:181-185 (2010).

[45] Vahdat, V., Ryan, K.E., Keating, P.L., Jiang, Y., Adiga, S.P., Schall, J.D., et al. Atomic-Scale Wear of Amorphous Hydrogenated Carbon during Intermittent Contact: A Combined Study Using Experiment, Simulation, and Theory. ACS Nano 8:7027-7040 (2014).

[46] Jacobs, T.D.B., Carpick, R.W. Nanoscale wear as a stress-assisted chemical reaction. Nature Nanotechnology 8:108-112 (2013).

[47] Shao, Y., Jacobs, T.D.B., Jiang, Y., Turner, K.T., Carpick, R.W., Falk, M.L. Multibond Model of Single-Asperity Tribochemical Wear at the Nanoscale. ACS Applied Materials & Interfaces 9:35333-35340 (2017).

[48] Sheehan, P.E. The wear kinetics of NaCl under dry nitrogen and at low humidities. Chemical Physics Letters 410:151-155 (2005).

[49] Cao, Z., Zhao, W., Liang, A., Zhang, J. A General Engineering Applicable Superlubricity: Hydrogenated Amorphous Carbon Film Containing Nano Diamond Particles. Advanced Materials Interfaces 4:1601224 (2017).

[50] Chen, L., Xiao, C., He, X., Yu, B., Kim, S.H., Qian, L. Friction and Tribochemical Wear Behaviors of Native Oxide Layer on Silicon at Nanoscale. Tribology Letters 65:139 (2017).

[51] Chen, L., Wen, J., Zhang, P., Yu, B., Chen, C., Ma, T., et al. Nanomanufacturing of silicon surface with a single atomic layer precision via mechanochemical reactions. Nature Communications 9:1542 (2018).

[52] Xiao, C., Xin, X., He, X., Wang, H., Chen, L., Kim, S.H., et al. Surface Structure Dependence of Mechanochemical Etching: Scanning Probe-Based Nanolithography Study on Si(100), Si(110), and Si(111). ACS Applied Materials & Interfaces 11:20583-20588 (2019).

[53] Xiao, C., Deng, C., Zhang, P., Qian, L., Kim, S.H. Interplay between solution chemistry and mechanical activation in friction-induced material removal of silicon surface in aqueous solution. Tribology International 148:106319 (2020).

[54] Xiao, C., Chen, C., Wang, H., Chen, L., Jiang, L., Yu, B., et al. Effect of counter-surface chemistry on defect-free material removal of monocrystalline silicon. Wear 426-427:1233-1239 (2019).

[55] Xiao, C., Li, J., Guo, J., Zhang, P., Yu, B., Chen, L., et al. Role of mechanically-driven distorted microstructure in mechanochemical removal of silicon. Applied Surface Science 520:146337 (2020).

[56] Li, Z., Szlufarska, I. Physical Origin of the Mechanochemical Coupling at Interfaces. Physical Review Letters 126:076001 (2021).

[57] Gao, J., Xiao, C., Feng, C., Wu, L., Yu, B., Qian, L., et al. Oxidation-induced changes of mechanochemical reactions at GaAs–SiO2 interface: The competitive roles of water adsorption, mechanical property, and oxidized structure. Applied Surface Science 548:149205 (2021).

[58] Raghuraman, S., Boonpuek, P., King, K.H., Ye, Z., Felts, J.R. The Role of Speed in Atomic Scale Wear. The Journal of Physical Chemistry C 125:4139-4145 (2021).

[59] Wang, K., Zhang, J., Ma, T., Liu, Y., Song, A., Chen, X., et al. Unraveling the Friction Evolution Mechanism of Diamond-Like Carbon Film during Nanoscale Running-In Process toward Superlubricity. Small 17:2005607 (2021).

[60] Boscoboinik, A., Olson, D., Adams, H., Hopper, N., Tysoe, W.T. Measuring and modelling mechanochemical reaction kinetics. Chemical Communications 56:7730-7733 (2020).

[61] Chen, X., Kawai, K., Zhang, H., Fukuzawa, K., Koga, N., Itoh, S., et al. ReaxFF Reactive Molecular Dynamics Simulations of Mechano-Chemical Decomposition of Perfluoropolyether Lubricants in Heat-Assisted Magnetic Recording. The Journal of Physical Chemistry C 124:22496-22505 (2020).

[62] Gosvami, N.N., Bares, J.A., Mangolini, F., Konicek, A.R., Yablon, D.G., Carpick, R.W. Mechanisms of antiwear tribofilm growth revealed in situ by single-asperity sliding contacts. Science 348:102-106 (2015).

[63] Zhang, J., Spikes, H. On the Mechanism of ZDDP Antiwear Film Formation. Tribology Letters 63:24 (2016).

[64] Ernens, D., Langedijk, G., Smit, P., de Rooij, M.B., Pasaribu, H.R., Schipper, D.J. Characterization of the Adsorption Mechanism of Manganese Phosphate Conversion Coating Derived Tribofilms. Tribology Letters 66:131 (2018).

[65] He, X., Ngo, D., Kim, S.H. Mechanochemical Reactions of Adsorbates at Tribological Interfaces: Tribopolymerizations of Allyl Alcohol Coadsorbed with Water on Silicon Oxide. Langmuir 35:15451-15458 (2019).

[66] He, X., Kim, S.H. Mechanochemistry of Physisorbed Molecules at Tribological Interfaces: Molecular Structure Dependence of Tribochemical Polymerization. Langmuir 33:2717-2724 (2017).

[67] He, X., Kim, S.H. Surface Chemistry Dependence of Mechanochemical Reaction of Adsorbed Molecules—An Experimental Study on Tribopolymerization of α-Pinene on Metal, Metal Oxide, and Carbon Surfaces. Langmuir 34:2432-2440 (2018).

[68] Johnson, B., Wu, H., Desanker, M., Pickens, D., Chung, Y.-W., Jane Wang, Q. Direct Formation of Lubricious and Wear-Protective Carbon Films from Phosphorus- and Sulfur-Free Oil-Soluble Additives. Tribology Letters 66:2 (2017).

[69] Ghanbarzadeh, A., Parsaeian, P., Morina, A., Wilson, M.C.T., van Eijk, M.C.P., Nedelcu, I., et al. A Semi-deterministic Wear Model Considering the Effect of Zinc Dialkyl Dithiophosphate Tribofilm. Tribology Letters 61:12 (2015).

[70] Akchurin, A., Bosman, R. A Deterministic Stress-Activated Model for Tribo-Film Growth and Wear Simulation. Tribology Letters 65:59 (2017).

[71] Dorgham, A., Parsaeian, P., Azam, A., Wang, C., Morina, A., Neville, A. Single-asperity study of the reaction kinetics of P-based triboreactive films. Tribology International 133:288-296 (2019).

[72] Singer, I.L., Bolster, R.N., Wegand, J., Fayeulle, S., Stupp, B.C. Hertzian stress contribution to low friction behavior of thin MoS2 coatings. Applied Physics Letters 57:995-997 (1990).

[73] Garvey, M., Weinert, M., Tysoe, W.T. On the Pressure Dependence of Shear Strengths in Sliding, Boundary-Layer Friction. Tribology Letters 44:67 (2011).

[74] He, X., Pollock, A., Kim, S.H. Effect of Gas Environment on Mechanochemical Reaction: A Model Study with Tribo-Polymerization of α-Pinene in Inert, Oxidative, and Reductive Gases. Tribology Letters 67:25 (2019).

[75] Chen, Z., Khajeh, A., Martini, A., Kim, S.H. Chemical and physical origins of friction on surfaces with atomic steps. Science Advances 5:eaaw0513 (2019).

[76] Chen, Z., Khajeh, A., Martini, A., Kim, S. Origin of High Friction at Graphene Step Edges on Graphite. ACS Applied Materials & Interfaces 13:1895–1902 (2020).

[77] Chen, Z., Khajeh, A., Martini, A., Kim, S.H. Identifying Physical and Chemical Contributions to Friction: A Comparative Study of Chemically Inert and Active Graphene Step Edges. ACS Applied Materials & Interfaces 12:30007-30015 (2020).

[78] Schwarz, U.D., Hölscher, H. Exploring and Explaining Friction with the Prandtl–Tomlinson Model. ACS Nano 10:38-41 (2016).

[79] Rigney, D.A., Hirth, J.P. Plastic deformation and sliding friction of metals. Wear 53:345-370 (1979).

[80] Klein, J. Shear, Friction, and Lubrication Forces Between Polymer-Bearing Surfaces. Annual Review of Materials Science 26:581-612 (1996).

[81] Ewen, J.P., Gao, H., Müser, M.H., Dini, D. Shear heating, flow, and friction of confined molecular fluids at high pressure. Physical Chemistry Chemical Physics 21:5813-5823 (2019).

[82] Barrie, P.J. The mathematical origins of the kinetic compensation effect: 2. the effect of systematic errors. Physical Chemistry Chemical Physics 14:327-336 (2012).

[83] Chen, L., He, H., Wang, X., Kim, S.H., Qian, L. Tribology of Si/SiO2 in Humid Air: Transition from Severe Chemical Wear to Wearless Behavior at Nanoscale. Langmuir 31:149-156 (2015).

[84] Chen, L., Yang, Y.J., He, H.T., Kim, S.H., Qian, L.M. Effect of coadsorption of water and alcohol vapor on the nanowear of silicon. Wear 332-333:879-884 (2015).

[85] Zhang, P., He, H., Chen, C., Xiao, C., Chen, L., Qian, L. Effect of abrasive particle size on tribochemical wear of monocrystalline silicon. Tribology International 109:222-228 (2017).